Multivalent recognition at fluid surfaces: the interplay of receptor clustering and superselectivity

Galina V. Dubacheva[Δ⊥‡*], Tine Curk[§‖‡], Daan Frenkel[†], and Ralf P. Richter[Δ#*]

[Δ]Biosurfaces Lab, CIC biomaGUNE, Paseo Miramon 182, 20014 Donostia - San Sebastian, Spain

[⊥]PPSM CNRS UMR8531, ENS Cachan, Université Paris-Saclay, 61 Avenue du Président Wilson, 94235 Cachan, France

[§]Institute of Physics, Chinese Academy of Sciences, Beijing 100190, People's Republic of China

[‖]Faculty of Chemistry and Chemical Engineering, University of Maribor, 2000 Maribor, Slovenia

[†]Department of Chemistry, University of Cambridge, Lensfield Road, Cambridge, CB2 1EW, United Kingdom

[#]School of Biomedical Sciences, Faculty of Biological Sciences, School of Physics and Astronomy, Faculty of Mathematics and Physical Sciences, and Astbury Centre for Structural Molecular Biology, University of Leeds, Leeds, LS2 9JT, United Kingdom

Supporting Information

1. Supporting Methods

1.1. Analytical model for the binding of multivalent probes to fluid and immobile surfaces

The case of immobile surfaces and low guest occupancy was treated in detail in our previous work.[1,2] We shall here first recapitulate the main features of this case, and then extend the theory, first to immobile surfaces and high guest occupancy, and then to fluid surfaces.

1.1.1. Binding to immobile surface at low guest occupancy

In a nutshell, a generalized Langmuir adsorption is used to treat the adsorption of polymers to the surface. The average number of adsorbed polymers in a lattice site is

$$\Theta(n) = \frac{\partial \ln \Xi(n)}{\partial(\beta\mu)} = \frac{\sum_{i=1}^{\infty} i z^i q_i}{1+\sum_{i=1}^{\infty} z^i q_i} \quad [S1]$$

where $z \cong \rho N_A a^3$ is the activity of polymers in solution (ρ is the molar density and N_A is Avogadro's number) and q_i is the bound partition function of i polymers at the lattice site of size a. $\beta^{-1} = k_B T$ with the Boltzmann constant k_B and the absolute temperature T defines the thermal energy. The grand partition function $\Xi(n) = 1 + \sum_{i=1}^{\infty} z^i q_i$ takes into account all possible numbers of polymers in the lattice site and $\mu = k_B T \ln z$ is the chemical potential of polymers in solution. For a single polymer, the bound partition function is the sum over all possible numbers of host-guest bonds λ weighted by the Boltzmann factor

$$q_1 = \sum_{\lambda=1}^{\lambda_{max}} e^{-\beta \tilde{F}(\lambda)} \binom{n}{\lambda} \binom{k}{\lambda} \lambda! \quad [S2]$$

with n and k being the number of guests on the surface of a lattice site and the number of hosts per polymer, respectively. $\lambda_{max} = \min[n, k]$ is the maximum number of possible formed bonds. The binding free energy of a polymer with λ formed bonds is

$$\tilde{F}(\lambda) = \lambda\, k_B T \ln(K_d\, a^3\, N_A) + \tilde{U}_{poly}(\lambda) \quad [S3]$$

with K_d being the dissociation constant between a single host and a single guest in solution and $\tilde{U}_{poly}(\lambda)$ being the entropic (configurational) cost to the polymer when λ bonds are formed.

The above equation can be well approximated by a binomial expansion if all important (non-negligible) terms in the sum of Eq. S2 satisfy $\lambda \ll n$ and the entropic (configurational) cost to the polymer is approximated to scale linearly with the number of bonds formed ($\tilde{U}_{poly}(\lambda) = \lambda U_{poly}$ with U_{poly} being a constant)

$$q_1 \approx \sum_{\lambda=1}^{\lambda_{max}} (n e^{-\beta F})^{\lambda} \frac{k!}{(k-\lambda)!\lambda!} = (1 + n e^{-\beta F})^k - 1 \quad [S4]$$

In this case, the single bond free energy is a constant for all bonds $F = k_B T \ln(K_d\, a^3\, N_A) + U_{poly}$. Finally, the partition function of the i^{th} polymer is obtained by assuming that the fraction of occupied guests remains low ($i\langle\lambda\rangle \ll n$, with $\langle\lambda\rangle$ being the average fraction of bonds per polymer) such that binding of different polymers can be treated as uncorrelated

$$q_i = \frac{1}{i!}\left[(1 + n e^{-\beta F})^k - 1\right]^i e^{-\beta U_i}. \quad [S5]$$

This expression was used in our previous studies.[1,2] All polymers within the lattice site were treated as independent and only interacting with each other through the mean-field repulsion U_i. The lattice size $a = R_g(4\pi/3)^{1/3}$ is determined by the polymer size R_g. For this lattice size, the repulsion term is $U_i = U_{pw} i + A_{dG} i^{9/4}$ accounting for the polymer/wall and polymer/polymer repulsion. The energy term for polymer/wall repulsion, $U_{pw} = 0.83\, k_B T$, was determined based on the size of the lattice a and the effective potential of mean force between a self-avoiding polymer and a wall.[2] Polymer/polymer repulsion assumed a Des

Cloiseaux law and the constant $A_{\mathrm{dG}} = 0.35k_{\mathrm{B}}T$ was obtained by fitting to experimental data.[1] We note that the condition $i\langle\lambda\rangle \ll n$ implies low guest occupancy.

1.1.2. Binding to immobile surface at high guest occupancy

We now generalize to the case when the approximation is not valid, i.e. $i\langle\lambda\rangle \ll n$ does not hold or $F(\lambda)$ is not linear. This is required, for example, in the case of high guest occupancy where the total number of bonds formed becomes comparable to the number of surface guests. Here, we need to consider the full expression which is rather complicated because now different polymers are not independent, *e.g.* if one polymer binds a certain guest then that guest is not available for the second polymer. Each polymer contributes one sum over the number of bonds it forms with the surface guests. Below we show the case of three polymers, $i = 3$,

$$q_3 = e^{-\beta U_3} \sum_{\lambda_1=1}^{k} \sum_{\lambda_2=1}^{k} \sum_{\lambda_3=1}^{k} e^{-\beta(\tilde{F}_1(\lambda_1)+\tilde{F}_2(\lambda_2)+\tilde{F}_3(\lambda_3))} \binom{k}{\lambda_1}\binom{k}{\lambda_2}\binom{k}{\lambda_3} \frac{n!}{(n-\sum\lambda_j)!}$$

However, the form is general for any number of polymers

$$q_i = e^{-\beta U_i} \prod_{j=1}^{i} \sum_{\lambda_j=1}^{k} e^{-\beta(\sum \tilde{F}_j(\lambda_j))} \binom{k}{\lambda_j} \frac{n!}{(n-\sum\lambda_j)!} \qquad \text{[S6]}$$

The upper bound on the sums was here extended to k. This generalization is allowed because the factorial of a negative number is infinity and all non-consistent terms are automatically zero. Using the above equation, we can calculate the average number of adsorbed polymers in a lattice site θ according to Eq. S1. Finally, this is averaged to take into account Poisson fluctuations in the number of guests per lattice site

$$p(n, n_0) = \frac{(n_0)^n}{n!} e^{-n_0} \qquad \text{[S7]}$$

where n_0 is the mean number of guests per site. The expected average number of adsorbed polymers per site thus becomes

$$\langle\Theta\rangle = \sum_{n=1}^{\infty} p(n, n_0)\Theta(n) \qquad \text{[S8]}$$

1.1.3. Fluid surface

Now let us consider the effect of surface guest mobility, which corresponds to 'annealed disorder' as opposed to 'quenched disorder' in the fixed case studied above. Above, we first calculated the number of adsorbed polymers and subsequently performed Poisson averaging (Eq. S8). In the annealed case, the system can relax internally within each lattice site and the Poisson averaging is done directly on a partition function.[3,4] The number of guests in a lattice site is fluctuating and the partition function (Eq. S7) has to be Poisson averaged

$$q_i^{\mathrm{mob}}(\bar{n}) = \sum_{n=1}^{\infty} p(n, \bar{n})\ q_i(\bar{n}) \qquad \text{[S9]}$$

with $\bar{n}$ being the mean number of free (non-bound) guests per lattice site. It is given by

$$\bar{n} = n_0 - \langle n_b\rangle \qquad \text{[S10]}$$

i.e. the mean free number of guests is determined by the mean total number per lattice site n_0, minus the number of guests $\langle n_b\rangle$ that are bound to the polymers. If individual host-guest binding is independent, $\tilde{U}_{\mathrm{poly}}(\lambda) = \lambda U_{\mathrm{poly}}$, and $\tilde{F}(\lambda) = \lambda F$, the Poisson averaging greatly simplifies the results and we get

$$q_i^{\mathrm{mob}}(\bar{n}) = \frac{1}{i!}\left[(1 + \bar{n}e^{-\beta F})^k - 1\right]^i e^{-\beta U_i} \qquad \text{[S11]}$$

which is the same expression that we obtained as an approximation for immobile guests (Eq. S5). The crucial difference is that Eq. S11 is exact if guests are non-interacting and Poisson distributed. The procedure of deriving Eq. S11 from Eqs. S9 and S6 is provided in our previous work.[4]

The average number of formed bonds can be computed by considering the grand partition function of

a single lattice site

$$\Xi^m(\bar{n}) = \sum_{i=1}^{\infty} {q_i}^{\mathrm{mob}}(\bar{n})\, z^i$$

The average number of bound guests can be obtained by the statistical mechanics relation

$$\langle n_b \rangle = \frac{\partial \ln \Xi^m(\bar{n})}{\partial(\beta\mu_G)} = \frac{\partial \ln \Xi^m(\bar{n})}{\partial \bar{n}}\bar{n}$$

with the free guest chemical potential $\beta\mu_{\mathrm{G}} = \ln \bar{n}$. Inserting this equation into Eq. S10 gives a self-consistent relation

$$\bar{n} = n_0 - \frac{\partial \ln \Xi^m(\bar{n})}{\partial \bar{n}}\bar{n} \qquad \text{[S12]}$$

that needs to be solved numerically (iteratively) to find the number of free (unbound) guests $\bar{n}$. This task is rather trivial because $\Xi^m(\bar{n})$ is a monotonically increasing function. After determining $\bar{n}$, we obtain the average number of adsorbed polymers per lattice site

$$\langle \Theta \rangle^{\mathrm{mob}} = \frac{\partial \ln \Xi^m(\bar{n})}{\partial(\beta\mu)} = \frac{\sum_{i=1}^{\infty} i z^i\, {q_i}^{\mathrm{mob}}(\bar{n})}{1+\sum_{i=1}^{\infty} z^i\, {q_i}^{\mathrm{mob}}(\bar{n})} \qquad \text{[S13]}$$

In the following we shall compare the fluid and immobile scenarios in some limiting conditions. As we shall see, this provides helpful constraints to understand how the shape of the binding curves differs between fluid and immobile scenarios.

1.1.4. Low/High binding limit (including Poisson fluctuations)

When adsorption is very low, most lattice sites are left empty ($\Theta \ll 1$). At sufficiently low Θ the average fraction of bound guests is also small, $\langle n_{\mathrm{b}} \rangle / n_0 \ll 1$, in which case we can approximate $\bar{n} \approx n_0$. Consequently, ${q_i}^{\mathrm{mob}}(\bar{n}) \approx {q_i}^{\mathrm{mob}}(n_0)$.

On the other hand, applying the limit $\Theta \ll 1$ in the immobile case, and using Eq. S1, we obtain $\sum_{i=1}^{\infty} i z^i q_i \ll 1$, from which we can approximate $\Theta \approx \sum_{i=1}^{\infty} i z^i q_i$. When we apply the Poisson averaging (Eq. S8), we have to compute essentially the same sum as in the fluid case (Eq. S9), the result of which is Eq. S11. Hence, in the low binding limit, both immobile and fluid guests yield the same adsorbed polymer surface density

$$\langle \theta \rangle \approx \langle \theta \rangle^{\mathrm{mob}} \approx \sum_{i=1}^{\infty} i z^i {q_i}^{\mathrm{mob}}(n_0) \qquad \text{[S14]}$$

In the opposite high binding limit all or at least most of the lattice sites are occupied ($\Theta \approx 1$) and excluded volume limits the deposition of more polymers. Hence, we again obtain that the binding curves for immobile and fluid guests must converge $\langle \theta \rangle \approx \langle \theta \rangle^{\mathrm{mob}}$.

The convergence in the low and high binding limits is also demonstrated by simulations (Fig. 4) as well as theoretical (Fig. 6) results.

1.1.5. Crossing-point between fluid and immobile binding curves

In addition, the experimental (Fig. 3), simulation (Fig. 4) and theoretical (Fig. 6) results indicate the existence of an intersection point in the adsorption curves when comparing immobile and fluid surfaces. Here we will demonstrate that this crossing-point, at which $\langle \theta \rangle = \langle \theta \rangle^{\mathrm{mob}}$, always exists.

Both the immobile (Eq. S1) and fluid (Eq. S13) adsorption curves are monotonically increasing functions of the number of guests n_0. In the low guest coverage limit the adsorbed polymer density is very low, the fraction of occupied guests is also very low and we can approximate $n_0 \approx \bar{n}$. In this regime the mobile (fluid) surface yields the larger adsorbed density $\langle \theta \rangle^{\mathrm{mob}} \geq \langle \theta \rangle$, where the equality holds in the limit $n_0 \to 0$.

To resolve the large n_0 regime we shall for clarity assume that at most one polymer can adsorb to any given lattice site. At very large n_0 all bonds would be satisfied $\langle n_b \rangle = k$ and Eq. S2 implies that $\bar{n} = n_0 -$

k. The fluid surface partition function, Eq. S11, becomes

$$q_1{}^{\mathrm{mob}} = \left[\left(1 + (n_0 - k)e^{-\beta F}\right)^k - 1\right] e^{-\beta U_1} \approx \left((n_0 - k)e^{-\beta F}\right)^k e^{-\beta U_1}. \quad [S15]$$

On the other hand the immobile partition function, from Eq. S6, is

$$q_1 = e^{-\beta U_1} \sum_{\lambda=1}^{k} e^{-\beta F \lambda} \binom{n}{\lambda} \binom{k}{\lambda} \lambda! \approx \frac{n!}{(n-k)!} e^{-\beta F k} e^{-\beta U_1}, \quad [S16]$$

where the approximation again assumes all bonds are satisfied $\lambda = k$. Since $\frac{n!}{(n-k)!} \geq (n_0 - k)^k$ at $n_0 = n$, the immobile partition function must be larger or equal than the fluid surface partition function, Eq. S11. Hence, there exists a regime where the adsorbed amount, from Eqs. S1 and S11, must be larger for immobile surfaces: $\langle\theta\rangle \geq \langle\Theta\rangle^{\mathrm{mob}}$, where the equality holds in the limit $n_0 \to \infty$.

Since $\Theta \geq \langle\Theta\rangle^{\mathrm{mob}}$ at large n_0, but $\langle\Theta\rangle^{\mathrm{mob}} \geq \langle\theta\rangle$ at small n_0, a crossing point must exist. In other words, the equation $\langle\Theta\rangle^{\mathrm{mob}} = \langle\theta\rangle$ generally has at least three distinct solutions. Two of these solutions were already described above: $n_0 \to 0$ and $n_0 \to \infty$. A third solution $n_0 = n^*$ defines the crossing point. These three guest surface densities at which $\langle\Theta\rangle^{\mathrm{mob}} = \langle\theta\rangle$ are also observed from the numerical simulation results in Fig. 4.

It is not straightforward to analytically predict the exact location of the crossing point. However, in the case of weak binding, $\langle n_{\mathrm{b}}\rangle / n_0 \ll 1$, we are able to estimate the location of the crossing point. Note that for clarity the unnecessary factor $e^{-\beta U_1}$ will be omitted in the calculations below. The immobile partition function (Eq. S2) is approximated by

$$q_1 \approx \frac{n_0!}{(n_0-\bar{\lambda})!\,(n_0)^{\bar{\lambda}}} \sum_{\lambda=0}^{\lambda_{\max}} e^{-\beta F \lambda} (n_0)^{\lambda} \binom{k}{\lambda} - 1 = \frac{n_0!}{(n_0-\bar{\lambda})!\,(n_0)^{\bar{\lambda}}} \left(1 + n_0 e^{-\beta F}\right)^k - 1, \quad [S17]$$

where $\bar{\lambda}$ denotes the mean number of formed bonds. The approximation is valid because the sum is peaked around $\bar{\lambda}$. On the other hand the fluid partition function (Eq. S11) is rewritten to

$$q_1{}^{\mathrm{mob}} = \left(1 + (n_0 - \langle n_{\mathrm{b}}\rangle)e^{-\beta F}\right)^k - 1 = \left(1 + n_0 e^{-\beta F}\right)^k \left(1 - \frac{\langle\theta\rangle\,\bar{\lambda}^2}{k\,n_0}\right)^k - 1, \quad [S18]$$

where we used the identity $\langle n_{\mathrm{b}}\rangle = \bar{\lambda}\langle\theta\rangle$ and $\bar{\lambda} \approx k \frac{n_0 e^{-\beta F}}{1 + n_0 e^{-\beta F}}$. Neglecting Poisson fluctuations, the crossing point is determined by $q_1 = q_1{}^{\mathrm{mob}}$, which yields

$$\frac{n_0!}{(n_0-\bar{\lambda})!\,(n_0)^{\bar{\lambda}}} = \left(1 - \frac{\langle\theta\rangle\,\bar{\lambda}^2}{k\,n_0}\right)^k.$$

Applying Stirling's approximation and the first order approximation of the exponential function we get

$$\frac{\bar{\lambda}}{n_0}\left(\bar{\lambda} - n_0 - 1/2\right) + \bar{\lambda} = \frac{\langle\theta\rangle\bar{\lambda}^2}{n_0},$$

and as the final result follows

$$\langle\theta\rangle = 1 - \frac{1}{2\bar{\lambda}}. \quad [S19]$$

The mean number of bonds per bound polymer is larger than one for multivalent binding: $\bar{\lambda} > 1$, therefore, the crossing point is located just below the saturation of the surface, $\langle\theta\rangle \sim 1$, and is, therefore, very close to the $n_0 \to \infty$ (or equivalently $\langle\theta\rangle = 1$) solution discussed above.

In deriving this result we have assumed at most one polymer is allowed per lattice site. However, the same result is obtained from numerical simulations shown in Fig. S4, where the regime of $\langle\theta\rangle^{\mathrm{mob}} \geq \langle\theta\rangle$ essentially covers the entire range of guest surface densities, except for very high and very low densities, and the crossing point is located close to surface saturation.

1.1.6. Model parameters

The analytical model contains two parameters which cannot be measured experimentally: the entropic contribution to the binding energy U_{poly} (Eq. S3) and the prefactor in a scaling approximation A_{dG} (Eq. S5). For HA with grafted β-CD as in the present work, we had determined $A_{dG} = 0.35\ k_BT$ and $U_{poly} = 4.6\ k_BT$ in our previous study.[2] These values were also used here to predict multivalent binding to immobile and fluid surfaces, while simultaneously tuning the characteristics of the multivalent probe.

1.1.7. Binding profile calculation tools

We provide an Excel spreadsheet with implemented analytical model valid at low guest occupancy (Eqs. S1-S5). This tool, which was also employed in our previous work[2], can be used for rapid prediction of multivalent polymer binding profiles.

Furthermore, a Matlab script is provided which calculates the binding profiles for immobile surfaces valid for any guest occupancy (Eqs. S6–S8). The script also determines the binding profiles for general fluid surfaces by iteratively converging to a self-consistent solution determined by Eqs. S9–S13.

1.2. Monte Carlo simulations

Grand canonical Monte Carlo simulations were performed using the soft blob model that we have described in detail in our previous work.[2] Here we extend the model to fluid surfaces. In order to capture the lateral diffusion of guests on the surface, we modified the Monte Carlo sampling such that in every Monte Carlo cycle a guest is chosen at random. If this guest is not bound to a polymer, a new location for the guest is chosen uniformly at random on the surface.[5] This modification does not interfere with our method of sampling multivalent interactions described in our previous work.[2]

The parameters used in our simulations were equal to that of our previous study.[2] The number of blobs per polymer was $m_b = 20$. Each simulation was run for $\sim 10^{11}$ MC cycles, where in each cycle we randomly selected either to insert or delete a polymer or to move a single blob. The blob-guest bond energy was fixed to $F = -3\ k_BT$, determined from our previous work for the HA-β-CD to AD binding.[2]

For the immobile surface exposed to HA with β-CD grafted at $n_{β\text{-}CD} = 187$, the data is averaged over 100 different random realizations of the surface guest positions.

2. Supporting Figures

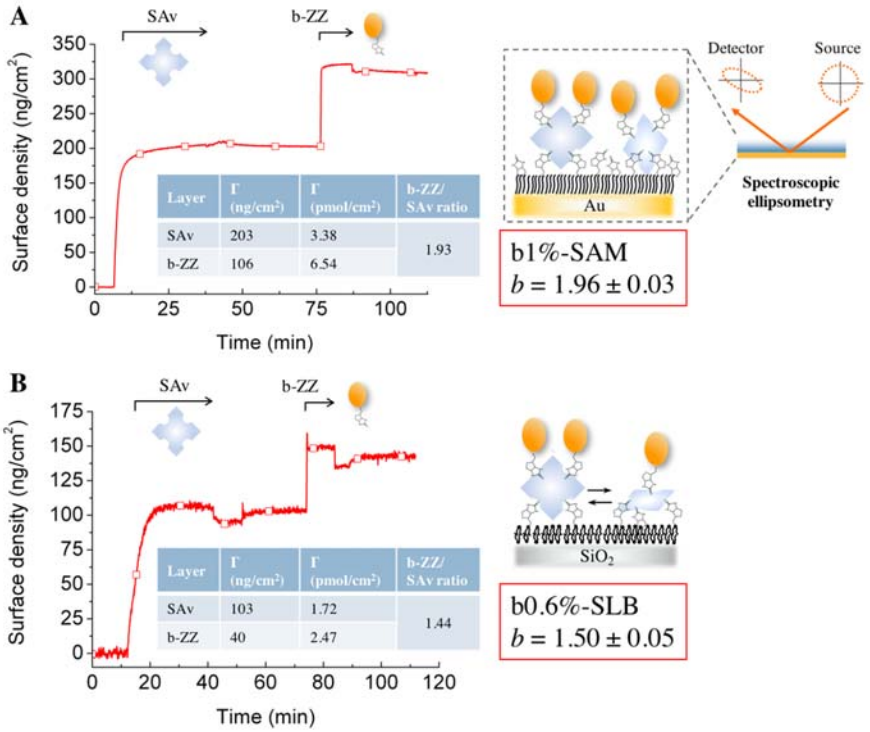

Figure S1. Quantification of SAv residual valency. Binding curves obtained by spectroscopic ellipsometry (SE) for the adsorption of SAv and the biotinylated reporter probe b-ZZ on b1%-SAM **(A)** and b0.6%-SLB **(B)**. Inset tables show the mass and molar surface densities of SAv and biotinylated probes, and the resulting b-ZZ/SAv ratio. The b-ZZ/SAv ratio is a measure of SAv residual valency, *i.e.*, the number of biotin binding sites available per molecule after engagement with the surface. All values were determined after protein adsorption and rinsing with working buffer once the SE response had stabilized. Schematics on the right illustrate the SE setup, and salient binding features, *i.e.* the typical orientations of SAv corresponding to the measured residual valencies: each SAv molecule engages with two biotins on the b1%-SAM, and with two or three biotins on the b0.6%-SLB; in the case of divalent binding, two distinct scenarios are possible (*cis* and *trans*) depending on the relative positions of the engaged biotin binding pockets[6] but these are not explicitly shown. The resulting residual valencies (b) are provided below the schematics as mean ± standard error, based on two independent measurements each. b-ZZ is a recombinant protein consisting of a tandem repeat of the Z domain of protein A connected through a flexible spacer (12 amino acids) to an N-terminal biotin. We have previously described the production and purification of b-ZZ, and demonstrated that b-ZZ is a faithful reporter of the residual valency of surface-bound SAv.[6] Conditions: 10 mM HEPES buffer (pH 7.4) with 150 mM NaCl; c_{SAv} = 10 µg/mL, $c_{b\text{-}ZZ}$ = 36 µg/mL, M_{SAv} = 60 kDa; $M_{b\text{-}ZZ}$ = 16.2 kDa; SAv adsorption time = 30 min, b-ZZ adsorption time = 10 min.

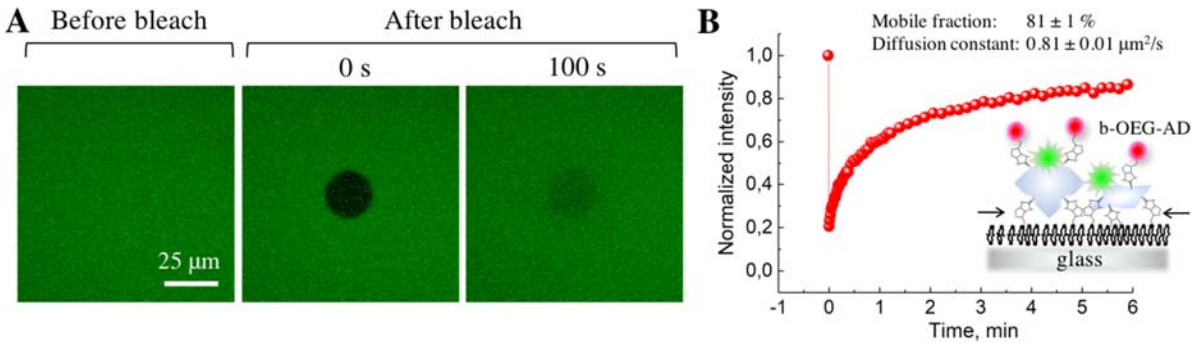

Figure S2. Characterization of guest lateral mobility by FRAP. FRAP measurements were performed using fluorescent SAv to report on the mobility of SAv-bound AD. Representative data are shown to illustrate the assay: b0.6%-SLB saturated first with SAv-atto565 and then with b-OEG-AD (see the experimental section of the manuscript for the details on the sample preparation). (**A**) Micrographs taken before and after photobleaching for a few seconds of a circular region of 20 µm diameter. (**B**) Kinetics of fluorescence recovery through lateral diffusion of SAv-atto565. The fluorescence intensity of the bleached spot, normalized against the fluorescence intensity of the non-bleached region of the same size (to correct for bleaching during image acquisition and drift effects) and background corrected for unbleached fluorescence, is plotted *versus* time**.** A schematic of the studied system is shown as inset.

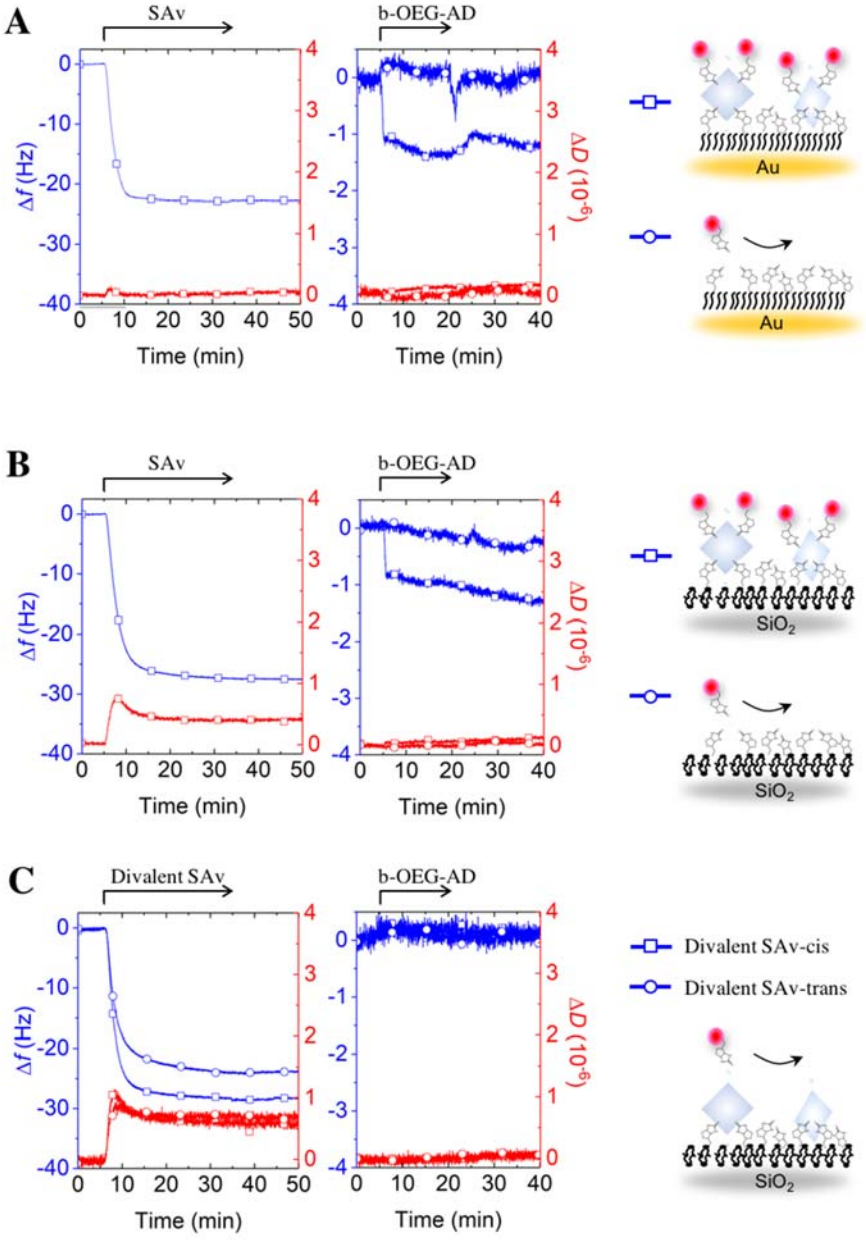

Figure S3. Specificity of b-OEG-AD/SAv interactions. Binding curves obtained by QCM-D for the adsorption of SAv and b-OEG-AD on b-SAMs **(A)** and b-SLBs **(B, C)**. Schematics on the right illustrate the main results: small but measurable decreases in frequency ($\Delta f \approx$ -1 Hz) indicate binding of b-OEG-AD to SAMs (**A**) or SLBs (**B**) that are functionalized with SAv (squares); in contrast, no significant responses are observed for b-OEG-AD on SAMs (**A**) or SLBs (**B**) lacking SAv (circles), and for b-OEG-AD on SLBs functionalized with SAv that lacks free biotin-binding sites (**C**). The assays in **C** were performed with two mutants of SAv in which two of the four biotin-binding sites are impaired: divalent SAv-cis (squares) retains two binding sites on the same face of the tetramer, and divalent SAv-trans (circles) two binding sites on opposite faces; both mutants bind divalently to the b-SLB albeit at different orientations (see ref. 6 for details). Conditions: biotinylation of SAMs = 10%, biotinylation of SLBs = 5%; 10 mM HEPES buffer (pH 7.4) with 150 mM NaCl; c_{SAv} = 10 µg/mL, $c_{b\text{-}OEG\text{-}AD}$ = 20 µg/mL, SAv adsorption time = 30 min, b-OEG and b-OEG-AD adsorption time = 15 min.

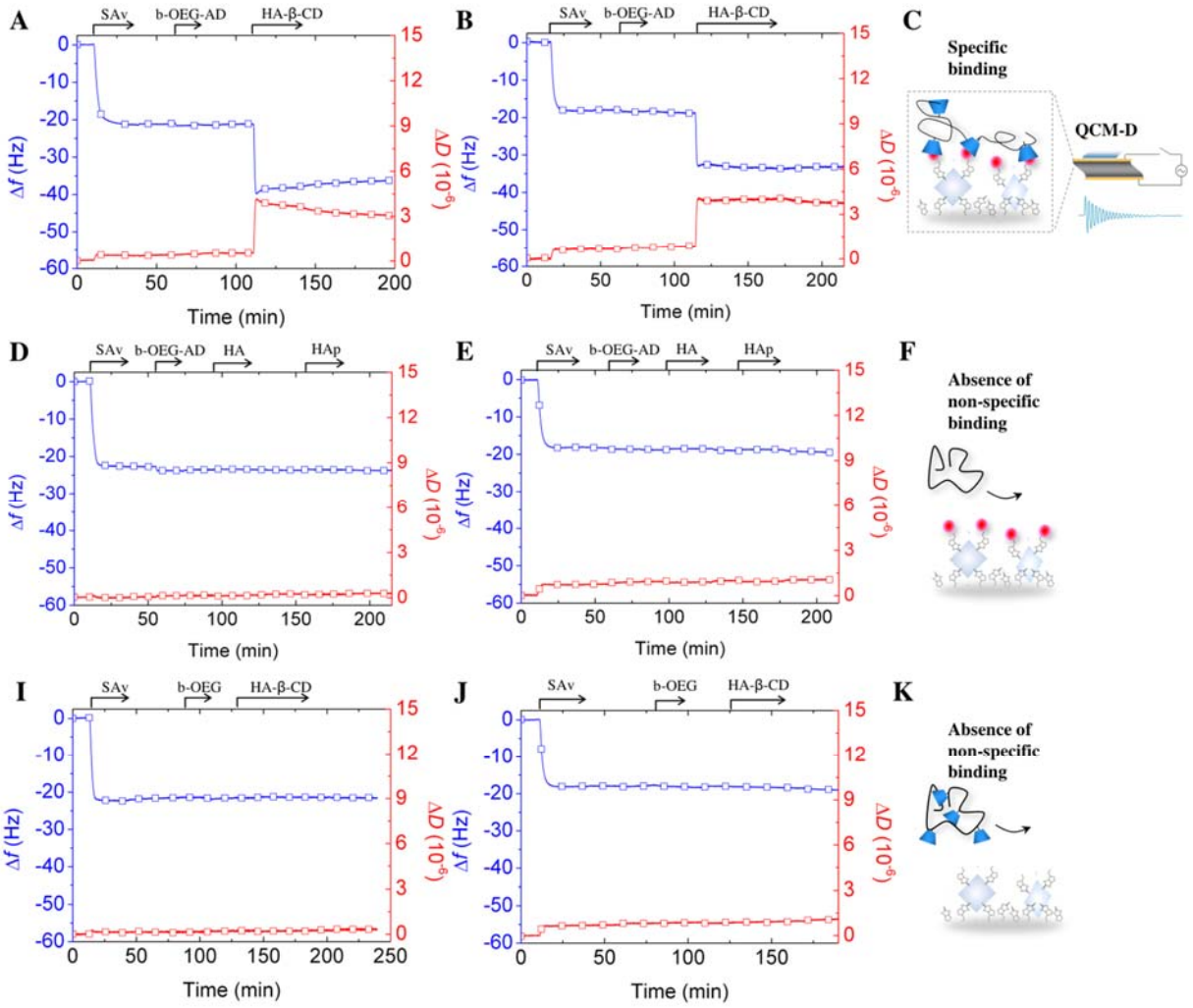

Figure S4. Specificity of multivalent β-CD/AD interactions. Binding curves obtained by QCM-D for the adsorption of SAv, biotinylated probes (b-OEG or b-OEG-AD) and HA constructs (HA, HA_p and HA-β-CD) on b-SAMs **(A, D, I)** and b-SLBs **(B, E, J)**; Schematics on the right **(C, F, K)** illustrate the main results: specific interactions between HA-β-CD and SAMs or SLBs displaying AD **(C)**, the absence of interactions between HA lacking β-CD and SAMs or SLBs displaying AD **(F)**, and the absence of interactions between HA-β-CD and SAMs or SLBs lacking AD **(K)**; in addition, the QCM-D setup is schematically shown in **(C)**. In previous work, we had already shown that SAv binding to b-SLBs and b-SAMs, and b-ZZ binding to SAv on b-SLBs or b-SAMs, is fully specific.[6] Molecules used for negative controls: plain and pentenoate-modified hyaluronan (HA and HA_p) are the precursors for the synthesis of HA-β-CD;[2] biotin-$(EG)_9$-amine (b-OEG) is the precursor for the synthesis of b-OEG-AD (see experimental section of the manuscript). Conditions: biotinylation of SAMs = 1%, except for **(D)** where b10%-SAMs were used, biotinylation of SLBs = 0.6%; 10 mM HEPES buffer (pH 7.4) with 150 mM NaCl; c_{SAv} = 10 µg/mL, $c_{b\text{-}OEG\text{-}AD}$ = $c_{b\text{-}OEG}$ = 20 µg/mL, $c_{HA\text{-}β\text{-}CD}$ = c_{HA} = c_{HAp} = 50 µg/mL, SAv adsorption time = 30 min, b-OEG and b-OEG-AD adsorption time = 20 min, HA, HA_p and HA-β-CD adsorption time = 30-60 min.

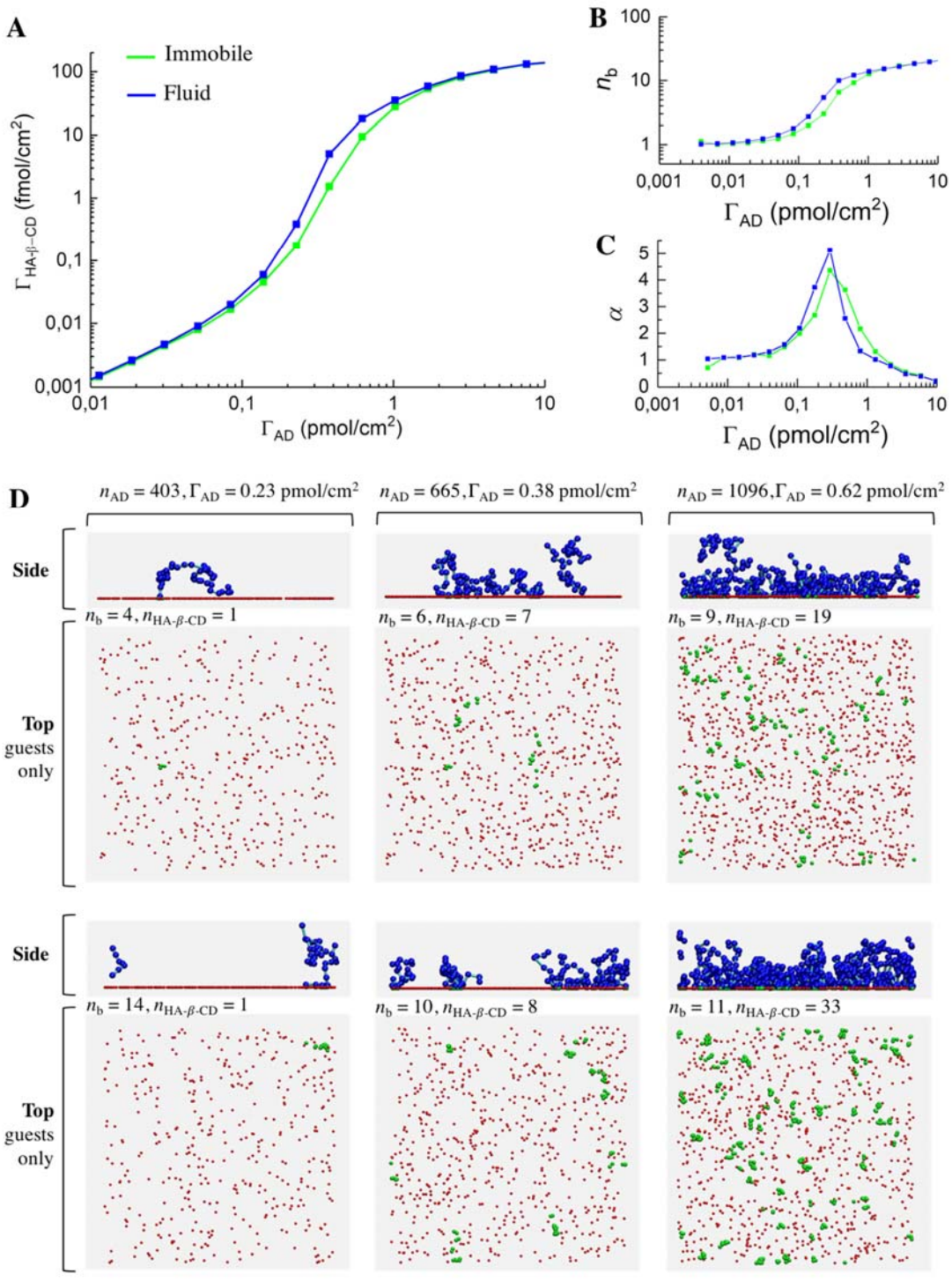

Fig. S5. At low guest occupancy, surface fluidity affects multivalent binding only marginally. Displayed are predictions from simulations for $n_{\beta\text{-CD}} = 27$ ($DS_{\beta\text{-CD}} = 3$ %, $M_w^{HA\text{-}\beta\text{-CD}} = 405$ kDa) using a simulation box of $L_x = L_y \approx 12 R_g^{HA\text{-}\beta\text{-CD}}$ with all other model parameters unchanged compared to the data shown in Fig. 4 in the main text; this corresponds to the regime of low guest occupancy. All data are displayed analogous to Fig. 4; in (A) to (C), each data point represents a single simulation run, and solid lines connect data points.

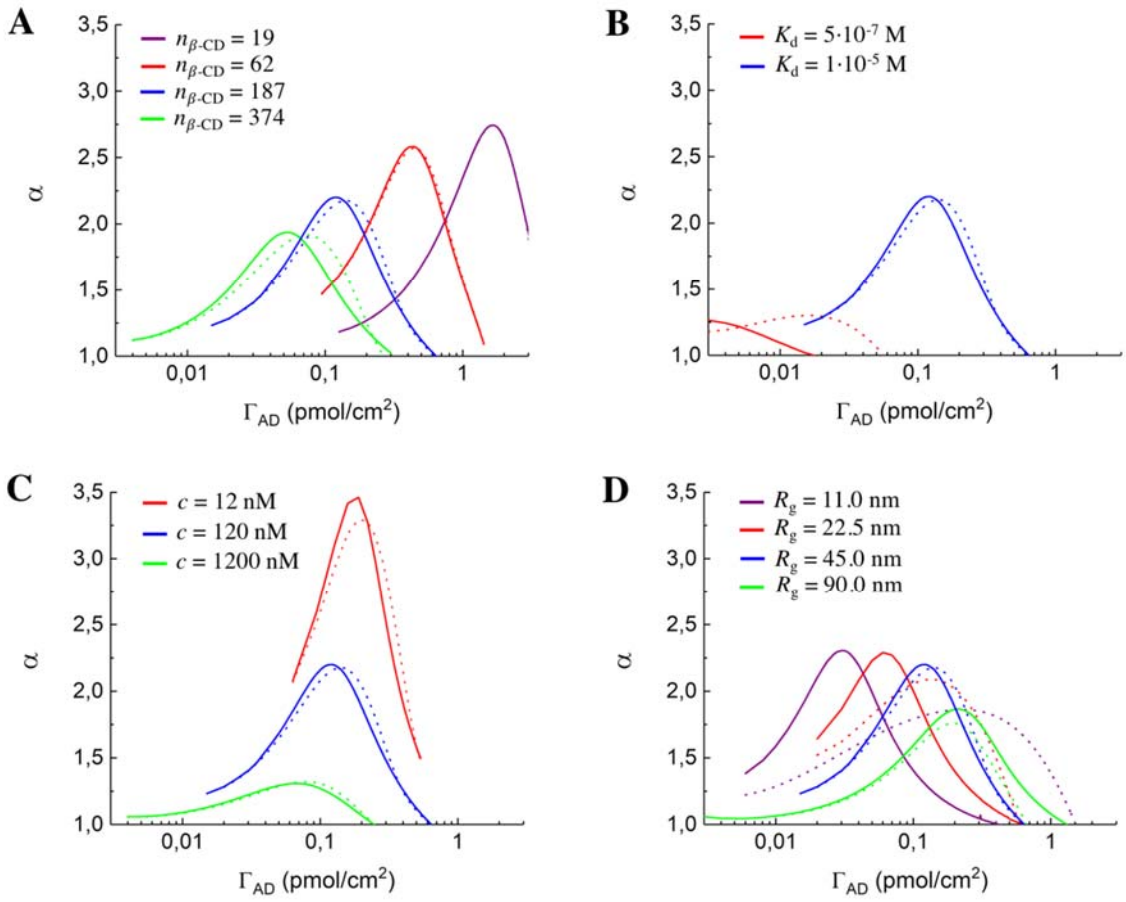

Fig. S6. Analytical modeling at tunable polymer characteristics. Superselectivity parameter, α, extracted from the theoretical data show in Fig. 6B-E and plotted *vs* Γ_{AD}. Analytical predictions are obtained for the fluid (solid) and immobile (dashed) cases at tunable $n_{\beta\text{-CD}}$ (A), K_d (B), c (C) and R_g (D). Blue curves in all graphs correspond to the reference system (Table 1).

3. Supporting References

(1) Dubacheva, G. V.; Curk, T.; Mognetti, B. M.; Auzély-Velty, R.; Frenkel, D.; Richter, R. P. Superselective Targeting Using Multivalent Polymers. *J. Am. Chem. Soc.* **2014**, *136* (5), 1722–1725.

(2) Dubacheva, G. V.; Curk, T.; Auzély-Velty, R.; Frenkel, D.; Richter, R. P. Designing Multivalent Probes for Tunable Superselective Targeting. *Proc. Natl. Acad. Sci.* **2015**, *112* (18), 5579–5584.

(3) Albertazzi, L.; Martinez-Veracoechea, F. J.; Leenders, C. M. A.; Voets, I. K.; Frenkel, D.; Meijer, E. W. Spatiotemporal Control and Superselectivity in Supramolecular Polymers Using Multivalency. *Proc. Natl. Acad. Sci. U. S. A.* **2013**, *110* (30), 12203–12208.

(4) Curk, T.; Dobnikar, J.; Frenkel, D. Optimal Multivalent Targeting of Membranes with Many Distinct Receptors. *Proc Natl Acad Sci USA* **2017**, *114* (28), 7210–7215.

(5) Frenkel, D.; Smith, B. *Understanding Molecular Simulation: From Algorithms to Applications*; Academic Press, Inc., 1996.

(6) Dubacheva, G. V.; Araya-Callis, C.; Geert Volbeda, A.; Fairhead, M.; Codée, J.; Howarth, M.; Richter, R. P. Controlling Multivalent Binding through Surface Chemistry: Model Study on Streptavidin. *J. Am. Chem. Soc.* **2017**, *139* (11), 4157–4167.